

## **Legends for supplementary figures:**

### **Supplementary Fig. 1. FoxO1-specific RNAi construct:**

**A:** Schematic representation of mouse FoxO1 cDNA. Three oligonucleotides that are complementary to FoxO1 cDNA 11-29 nt, 814-832 nt, and 1381-1399 nt were used for RNAi constructs. **B:** FoxO1-RNAi expression plasmid vector. Two complementary oligonucleotides encoding two identical 19-bp RNAi sequences in a head-to-head orientation with 9 nucleotides in between and with two 3'-UU overhangs were synthesized, according to the manufacturer's instruction (Ambion, Austin, TX). In addition, an Apol site and an EcoRI site were included in the upstream and downstream of the DNA oligos for facilitating DNA cloning. After self-annealing of two single complementary DNA, the resulting double-stranded DNA was cloned into pSilencer 2.0-U6 plasmid. Likewise, all three FoxO1-RNAi species were respectively cloned under the control of mouse U6 promoter and were subsequently confirmed by DNA sequencing, using the 2.0rev primer (5'-AGGCGATTAAGTTGGGTA-3', Ambion).

### **Supplementary Fig. 2. Effect of FoxO1-RNAi on blood glucose metabolism:**

C57BL/6J mice (Male, 12-wk old, Jackson Laboratory) were stratified by body weight and randomly assigned to four groups (n=6) to ensure a similar mean body weight. Mice were intravenously injected with 3-ml saline containing 5  $\mu$ g of control pSilencer 2.0-U6 plasmid DNA or 5  $\mu$ g of RNAi plasmid vector encoding each of the three FoxO1-RNAi species under control of the mouse U6 promoter, as described in supplementary Fig. 1. We used an established hydrodynamic gene transfer approach for delivering FoxO1-RNAi into livers of mice, as described (40). Fasting blood glucose levels were determined at day 3 after a 15-h fast (**A**), and compared to nonfasting blood glucose

levels at day 2 under nonfasting conditions (**B**). Data were shown for FoxO1-RNAi (11-29 nt), as other two FoxO1-RNAi constructs did not result in significant changes in blood glucose levels under both fasting and nonfasting conditions three days after DNA administration. \* $P < 0.01$  vs. control by ANOVA.

**Supplementary Fig. 3. Effect of FoxO1-RNAi on hepatic gene expression:**

Mice were sacrificed under fasting conditions three days after FoxO1-RNAi (11-29 nt) plasmid vector administration. Liver tissues were collected for the preparation of total hepatic RNA, which was subjected to real time qRT-PCR analysis using specific primers corresponding to FoxO1, PEPCK, G6Pase, and  $\beta$ -actin mRNA, as described (33).

Hepatic abundance of FoxO1 (**A**), PEPCK (**B**) and G6Pase (**C**) mRNA relative to  $\beta$ -actin mRNA was compared between control and FoxO1-RNAi groups. \* $P < 0.05$ , and \*\* $P < 0.001$  vs. control by ANOVA.

**Supplementary Fig. 4. Hepatic MTP production and plasma TG levels in obesity and *db/db* mice:**

Male C57BL/6J mice of 8 weeks old were fed a high fat diet (n=6) and regular chow (n=6) for 8 weeks, followed by the determination of plasma TG (**A**) and cholesterol (**B**) profiles by FPLC column chromatography. VLDL, LDL/IDL and HDL peaks were indicated in A and B. At the end of 8-wk treatment, mice were sacrificed and liver tissues were subjected to semi-quantitative immunoblot assay for the determination of hepatic MTP levels (**C**). Likewise, plasma TG (**D**) and cholesterol (**E**) levels were determined in male diabetic *db/db* mice (n=6, 6-month old) and age-/sex-matched heterozygous *db/+* control littermates (n=6). Hepatic MTP levels in diabetic *db/db* and control *db/+*

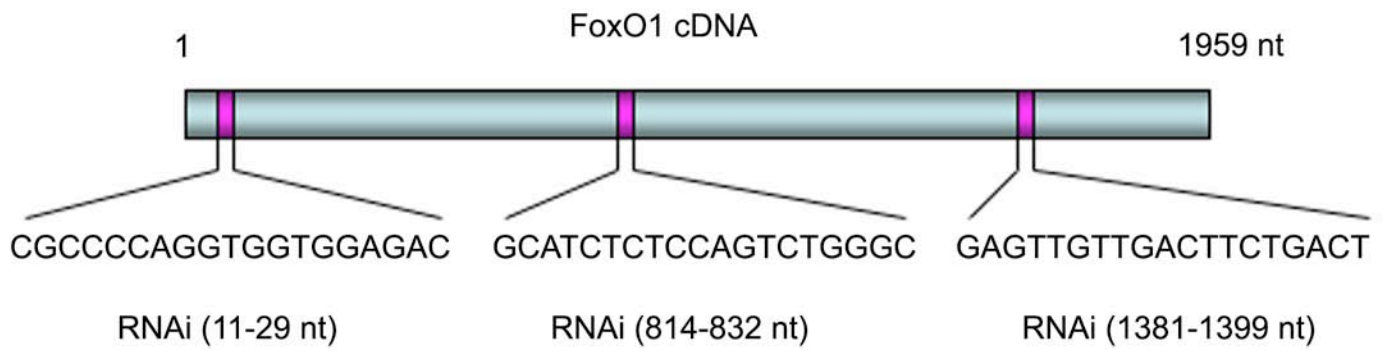
littermates were determined by semi-quantitative immunoblot assay using anti-MTP and anti-actin antibodies (**F**). \* $P < 0.05$  vs. control.

**Supplementary Fig. 5. Comparison of hepatic FoxO1 and Foxa2 subcellular distribution in obese *db/db* mice:**

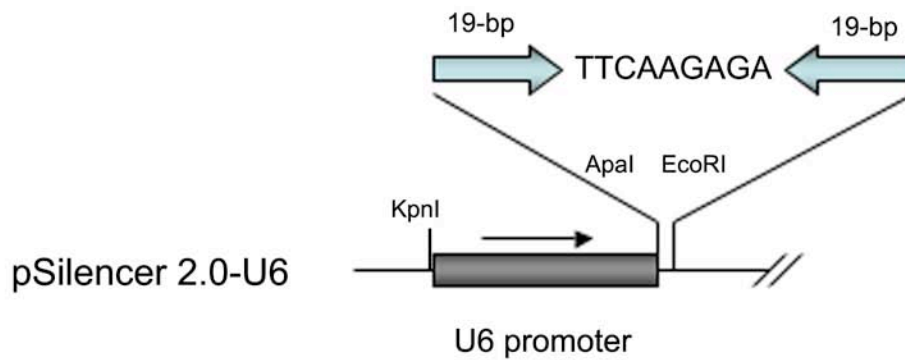
**A:** Western blots of FoxO1 and Foxa2. Liver tissues (20 mg) of male diabetic *db/db* mice (n=6, 6-month old) and age-/sex-matched heterozygous *db/+* control littermates (n=6) were homogenized for the preparation of cytoplasmic and nuclear fractions. Aliquots of proteins (20  $\mu$ g) were subjected to immunoblot analysis using anti-FoxO1 and anti-Foxa2 antibodies, respectively. Anti-actin antibody was used as control. **B:** Subcellular distribution of FoxO1 in liver. Hepatic FoxO1 distribution was predominantly cytoplasmic in lean control mice, but became nuclear in obese *db/db* mice. **C:** Subcellular distribution of Foxa2 in liver. Unlike FoxO1, Foxa2 was localized predominantly in the nucleus in both lean and obese *db/db* mice. The relative abundance of FoxO1 (or Foxa2) in cytoplasmic vs nuclear fractions, and total FoxO1 (or Foxa2) proteins in liver of obese *db/db* and control littermates were determined by densitometry using actin as an internal control. \* $P < 0.01$  by ANOVA.

Supplemental Fig. 1

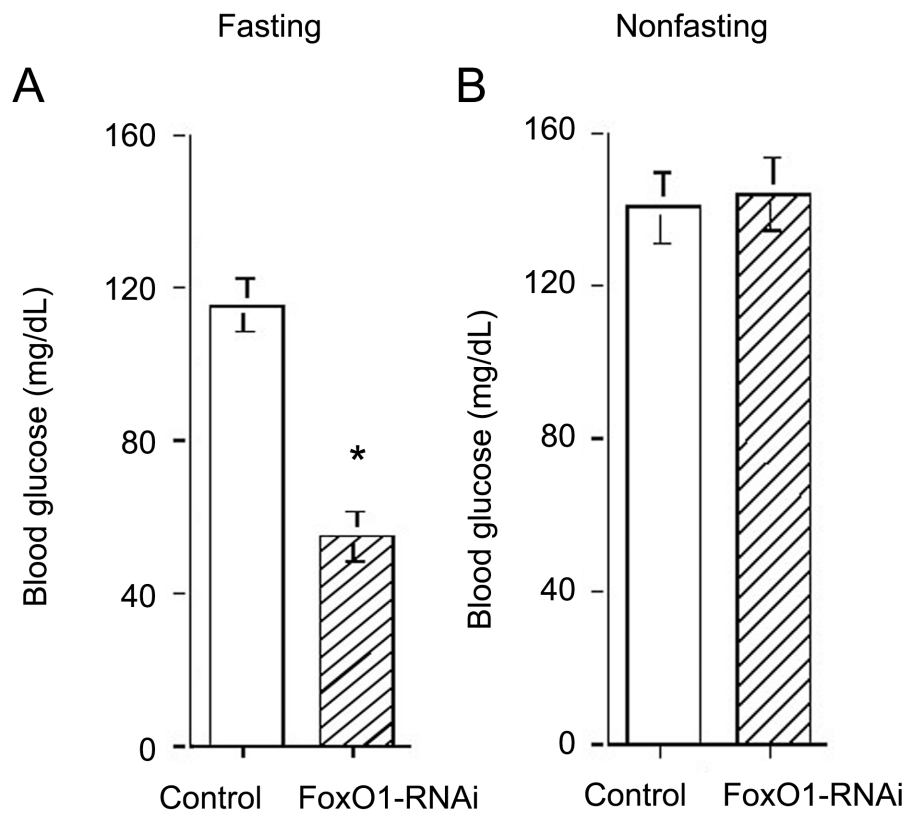
A



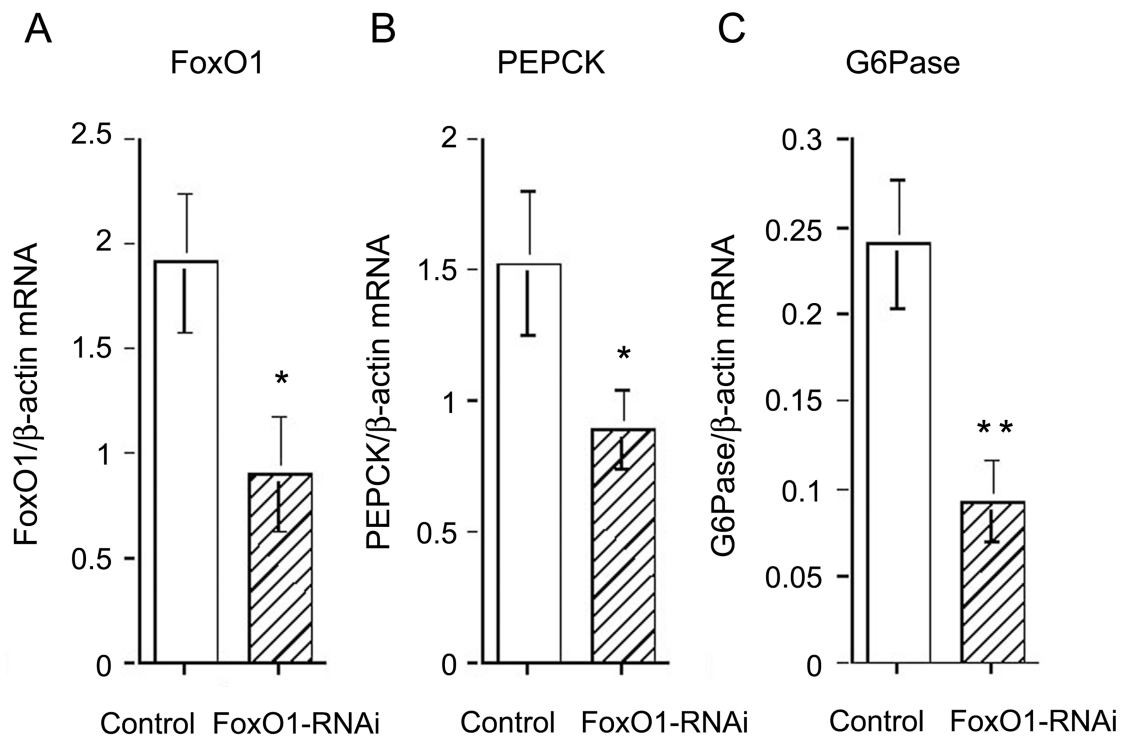
B



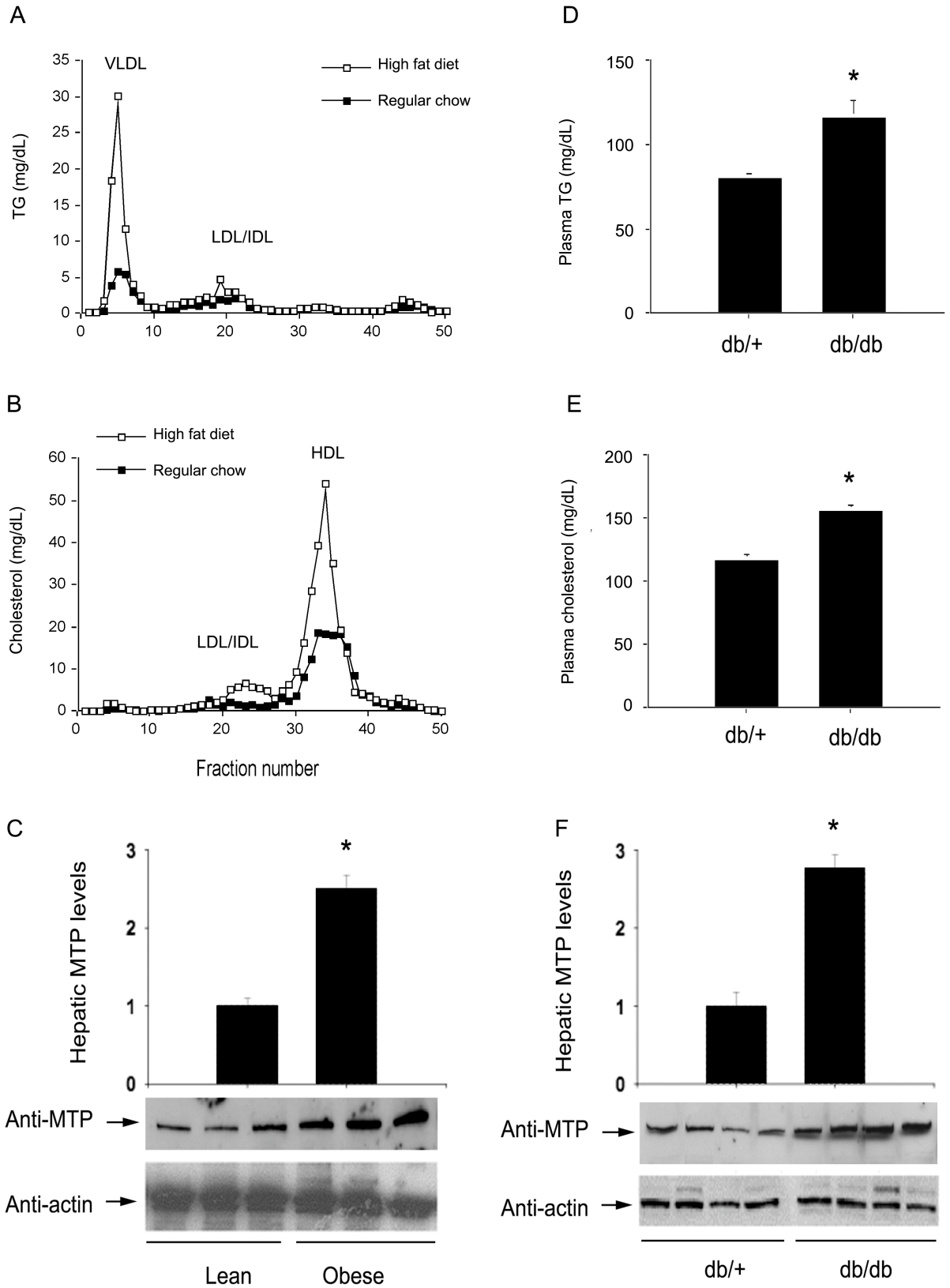
Supplemental Fig. 2



Supplementary Fig. 3



Supplementary Fig. 4



Supplementary Fig. 5

